Anal. Bioanal. Electrochem., Vol. 12, No. 3, 2020, 318-328

Analytical & Bioanalytical Electrochemistry

www.abechem.com

Full Paper

Synthesis, Structure and Catalytic Performance of N_4-Macrocycles of Fe^{III} and Co^{II} for Oxidation of Hydroquinone

Vinod Kumar Vashistha, Deepak Kumar Das, Anubha Yadav, Deepak Saini, and Anuj Kumar*

Department of Chemistry, Institute of Applied Science & Humanities, GLA University, Mathura, India

*Corresponding Author, Tel.: +91-8923302899

E-Mail: anuj,kumar@gla.ac.in

Received: 6 February 2020 / Received in revised form: 20 March 2020 / Accepted: 21 March 2020 / Published online: 31 March 2020

Abstract- Macrocycles and p-benzoquinones (p-BQ) have been generally connected as potential co-synergist redox models in aerobic oxidation. To get insight for the synergist oxidation of hydroquinones (H_2Q), thus, we synthesized and characterized dibenzotetraaza [14]annulene type macrocycles of Fe^{III} and Co^{II} metal ions and described by utilizing different examinations including molar conductance, IR, UV-Vis, mass and cyclic voltammetric measurements. The spectroscopic and computational studies proposed that the macrocycles have saddle shape distorted octahedral structure. These macrocycles demonstrated the reversible and quasi-reversible redox process pursued by Randles-Sevcik equation, demonstrating the adjustment of unusual oxidation conditions of metal ions. Further, the experimental consequences presented herein enlighten the catalytic activity of these macrocycles towards the oxidation of H_2Q. The results indicated that in the absence of macrocycles, the molecular oxygen is inactive with H_2Q but in presence of synthesized macrocycles H_2Q initiates prompt oxidation with the production of H_2O_2. Moreover, Co^{II} macrocycle was found to be an efficient catalyst for the oxidation of H_2Q into corresponding benzoquinones.

Keywords- Fe^{III}/Co^{II} Macrocycles; Template synthesis; CV and Catalytic Oxidation; Hydroquinones

1. INTRODUCTION

Naturally occurring N_4-macrocyclic complexes such as porphyrin and corrin ring have been

investigated as the possible alternative catalysts for enzymes in many oxidation and hydroxylation reactions [1-3]. Many successful efforts have also been made to synthesize similar N_4-macrocycles such as cyclam [4], cyclen [5], phthalocyanine [6], and other macrocyclic complexes [7]. These macrocycles are considered well-suited models for naturally occurring macrocyclic systems due to a stable N_4 environment whose coordination chemistry closely resembles that of porphyrin and corrin ring in their structure and functional relationships [8]. A large number of macrocyclic complexes are highly conjugated and exhibit extensive electron delocalization. Macrocycles with conjugation have more interaction with metal orbital and affect the cavity size. Such effects are more influenced in [14]-membered macrocycles that encapsulate metal ion and stabilize unusual oxidation state [9].

Further, the synthetic macrocycles and benzoquinones (BQs) were employed as potential co-catalytic redox mediators in homogeneous aerobic oxidation reactions [10]. Usually, these reactions involve the oxidation of (i) hydroquinones H_2Q mediated by the oxidizing catalyst, and (ii) reducing catalyst by O_2. In this process, mediators make possible the use of oxygen as the terminal oxidant [11]. Co(salophen) metal complex has been proven as the common co-catalysts for the Palladium derived catalysts and other catalytic aerobic oxidation reactions. The mechanism of Co(salophen) catalyzed the oxidation of H_2Q was demonstrated largely with catechol substrates (specifically, *o*-H_2Q), such as 3,5-di-tert-butylcatechol [12]. The significance of these studies to the oxidation of H_2Q to p-BQ is still unclear, because catechols normally chelate the metal center, and this coordination approach is not handy to H_2Q [13]. The results highlighted the function of H-atom and proton-coupled electron transfer steps in the O_2 reduction succession and proposed that H_2Q could assist to keep away from formation of side products in aerobic oxidation reactions by helping as "anti-oxidants" that cut off active O_2 species [14,15].

In this work, synthesis and characterization of [14]-membered N_4 macrocyclic complexes of Fe^{III} and Co^{II} have been carried out. In addition, electrochemical studies were also performed using cyclic voltammetry. Further, the catalytic oxidation of H_2Q was taken into investigation and the results showed that these macrocycles can be utilized as potential models for the catalytic oxidation of H_2Q.

2. EXPERIMENTAL

2.1. Material and methods

All the chemicals and solvents were purchased from TCI, India and used without further purification. The FT-IR spectral studies were carried out on Shimadzu 8400S spectrophotometer (4000- 400 cm^{-1}) by using KBr/DRS system. UV-vis spectra were recorded on a Shimadzu 2550 spectrophotometer (200-800 nm) using ethanol as a solvent. The molar conductance was measured on auto-ranging Conductivity/TDS Meter TCM 15+ instrument

using conc. 10^{-3} M in acetonitrile. Cyclic Voltammetric studies were performed on PGSTAT 101 Autolab Metrohm model 663 VA stand using three electrode system consisting of Pt disc as a working electrode (0.031cm^2), Ag/AgCl (KCl) as reference electrode, Pt wire as a counter electrode. Tetraethylammonium perchlorate (TEAP) used as supporting electrolytes in the experiment. Elemental analysis and Mass studies (LC-MS) was performed at CIL SAIF, Panjab University, Chandigarh.

2.2. Synthesis and characterization of macrocycles

The N_4-macrocycles of Fe^{III} and Co^{II} metal ions were synthesized by the template method [16] as illustrated in Scheme 1. Typically, 4-diaminobenzene (0.002 mol), acetylacetone (0.002 mol) and metal salt $FeCl_3.6H_2O$ (0.001 mol) {for complex A} OR $CoCl_2.2H_2O$ (0.001 mol) {for complex B} were taken in a round bottom flask containing 100 mL ethanol solvent. Then the reaction mixture was refluxed at 90 ^oC with medium stirring for about 10 h. The purity of the complexes was checked by using TLC. The dark brown colored crystals were collected, washed and finally with ethanol, acetone, diethyl ether, ethanol, and dried in a vacuum oven at 60 ^oC and characterized by multiple spectroscopies. The molecular formulae for the macrocyclic complexes have been assigned on the basis of elemental analysis and mass spectral data. The data remarkably support the expected reaction and product macrocyclic complexes. Thus, these macrocycles may be formulated as $[Fe(L)Cl_2]Cl$ (A), and $[Co(L)Cl_2]$ (B), where L is N_4-macrocyclic ligand ($C_{22}H_{24}N_4$). The analytical data for both macrocycles is given in Table 1.

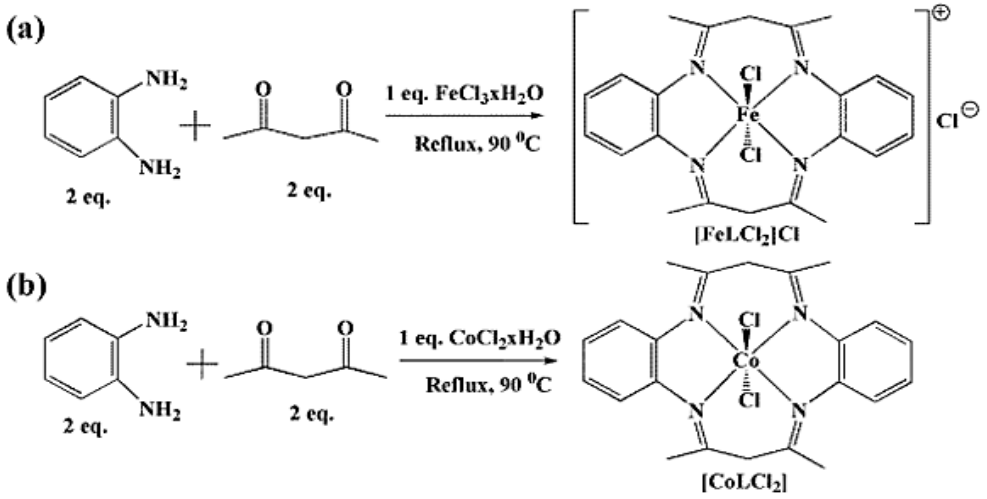

Scheme 1. Synthesis scheme of the Complex (a) A, and (b) B

Table 1. Analytical data, FT-IR and Electronic data of the prepared macrocycles

Micro-analytical Data					
Macrocycles (M. Wt.)	**Color**	**M. Cond.** (ohm^{-1} cm^2 mol^{-1})	**Microanalysis % found (calculated)**		
			C	**H**	**N**
A (470.25)	Dark brown	**32**	52.15 (52.01)	04.77 (04.33)	11.06 (11.16)
B (473.12)	Brown	**15**	55.71 (55.11)	05.10 (05.02)	11.81 (11.53)
FT-IR Spectral Data					
Macrocycles	***ν*(C=N) cm^{-1}**		***ν* (-C-H(CH_3)) cm^{-1}**	***ν* (C=C) cm^{-1}**	***ν* (M-N) cm^{-1}**
A	1634		2830,1450,	1615	472
B	1640		2835, 1446,	1590	476
Electronic Spectral Data					
Macrocycles	**Absorption (cm^{-1})**		**Band assignment**	**Geometry**	**Є (dm^3mol^{-1} cm^{-1})**
A	26666 cm^{-1} 17391 cm^{-1} 15384 cm^{-1}		$^6A_{1g}\rightarrow{}^4T_{1g}(F)$ $^6A_{1g}\rightarrow{}^4T_{1g}(P)$ $^6A_{1g}\rightarrow{}^4T_{2g}(P)$	Octahedral	165 82 79
B	28169 cm^{-1} 17543 cm^{-1} 14705 cm^{-1}		$^4T_{1g}\rightarrow{}^4T_{2g}(F)$ $^4T_{1g}\rightarrow{}^4A_{2g}(F)$ $^4T_{1g}\rightarrow{}^4T_{1g}(P)$	Octahedral	161 90 46

3. RESULTS AND DISCUSSION

3.1. Fourier transform infrared spectroscopy (FT-IR) studies

FT-IR spectral studies were performed to confirm the structural features in the macrocycles. FT-IR spectra of both macrocycles showed no featured band of free *ν* (C=O) and primary amine *ν* (NH_2), suggesting to the complete condensation reaction. While, the FT-IR spectra, showed the C-H (-CH_3) and C=N stretching vibration at 2900 cm^{-1} and 1632-1640 cm^{-1}, respectively [17].

The lower value of the frequency of ν (C=N) vibrations are elucidated by a drift of the lone pair electron density of the azomethine nitrogen towards the metal atom as well as due to the extension of conjugation with the aromatic ring, signifying that coordination takes place through the nitrogen of the C=N groups. Further, a weak absorption band in the region 3030-3100 cm^{-1} and 1461-1617 cm^{-1} allocated to Ar-H stretching vibration and -C=C stretching frequency, respectively. The FT-IR data for both macrocycles are presented in Table 1.

3.2. Ultraviolet-visible spectroscopic (UV-vis) studies

The electronic absorption spectra of the macrocycles were recorded at room temperature in 10^{-3} M solution in methanol with the range of 200-800 nm. The absorption band near 250 and 285 nm is due to $\pi \rightarrow \pi^*$ and $n \rightarrow \pi^*$ transition, respectively [18]. The electronic spectra of complex A showed three bands at ν_1 = 15384 cm^{-1} (650 nm, 79 dm^3mol^{-1} cm^{-1}), ν_2 = 18518 cm^{-1} (540 nm, 82 dm^3mol^{-1} cm^{-1}) and ν_3 = 28169 cm^{-1} (355 nm, 165 dm^3mol^{-1} cm^{-1}) that indicate transitions $^6A_{1g} \rightarrow {}^4T_{1g}$ (F), $^6A_{1g} \rightarrow {}^4T_{1g}$ (P), and $^6A_{1g} \rightarrow {}^4T_{2g}$ (P), respectively. Whereas, the electronic spectra of complex B showed spin allowed bands at, ν_1 = 14705 cm^{-1} (680 nm, 161 dm^3mol^{-1} cm^{-1}), ν_2 = 17543 cm^{-1} (570 nm, 46 dm^3mol^{-1} cm^{-1}) and ν_3 = 26666 cm^{-1} (375 nm, 90 dm^3mol^{-1} cm^{-1}) [19]. On the basis of the bands observed, a distorted octahedral geometry can be assigned to the complexes and may acquire D_{4h} symmetry. The assignment of octahedral geometry for these macrocycles also supported by the value of (ν_2/ν_1) ratio = 1.2, which is close to the expected value for octahedral geometry. Further, the value of molar conductance, measured in DMSO, for the complex A was found to be 32 ohm^{-1} cm^2 mol^{-1}, showing it to be 1:1 complex, where two chloride ions are at axial positions and the third chloride ion is located at outside of coordination sphere. In a similar way, the very low value of molar conductance (15 ohm^{-1} cm^2 mol^{-1}) for the complex B showed the non-electrolyte nature and the axial positions being possessed by two chloride ions [20]. The electronic spectral data for both macrocycles is given in Table 1.

.

3.3. Mass spectra

The LC-MS spectra for these macrocycles were recorded in positive ion mode. The mass spectra of complexes A and B demonstrated the molecular ion peaks at m/z 470.25 and 473.12, indicating the formation of macrocycles, respectively [21]. Many other fragments were also observed in the spectra which characterizes the composition of these synthesized macrocycles. These results are in good agreement with respect to their molecular formula of the macrocycles.

3.4. Computational Study

The density functional theory (DFT) was also taken into account to understand and propose the structure of these macrocycles. The geometry optimization in the gas phase with default convergence criteria was performed using hybrid functional B3LYP in conjunction with Pople's split-valence double-zeta polarised basis set, 6-31G*. Theoretical computations were executed for all probable spin states to establish the ground state conformation of proposed structures to these macrocycles. The vibrational frequencies of the optimized structures were also determined to generate VZPE (vibrational zero-point energy) corrections. Also, the absence of imaginary frequency confirmed the optimized geometries to be on the minima of their potential energy surfaces. Taking into consideration the geometric parameters of the

macrocycles, the M-N bond lengths (M=Metal) for all the spin states were studied and the optimized structure of these macrocycles is shown in Figure 1. These results showed the 'saddle shape' structure of this macrocycle which may occur due to the steric repulsion of the benzenoid moiety with $–CH_3$ groups on the macrocyclic framework. The resulting strain is alleviated by twisting of the torsional angles about the C-N bonds on the macrocyclic framework, which is the most easily distortable site. This alteration of the ring provides a nonplanar structure. The degree of departures from the dihedral angle in a preferably planar structure depends on the single and double bond character of the different bonds in the macrocyclic ring. In the 'saddle shape,' the lone pairs on N are pointed out of the N_4-plane so that the metal "sits atop" and not in the interior the N_4 cavity. In view of the fact that the macrocycle is crinkled and the metal ion is directing outside the N_4-plane on the side reverse to the folding, it is fairly pictured so as to support the coordination of the axial ligand [22].

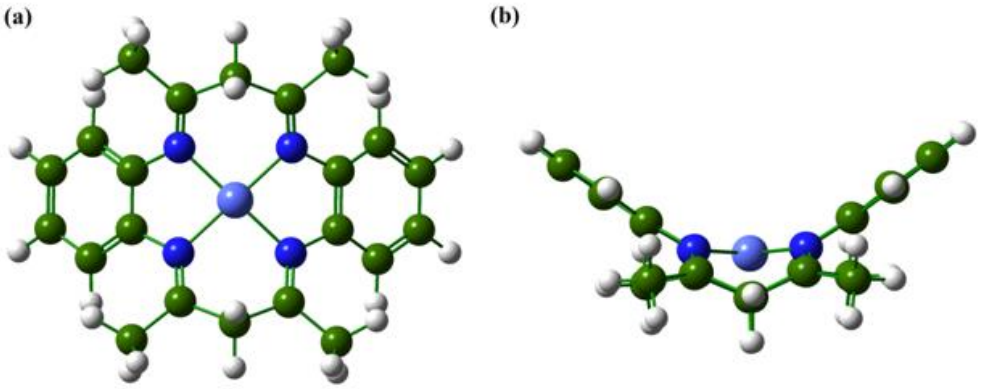

Fig. 1. The optimized structure of complex B (a) top view, and (b) side view

3.5. Redox studies

The redox behavior of the prepared macrocycles was evaluated by cyclic voltammetric measurements in the DMF solution having 10^{-3} M concentration of each macrocycle and 0.1 M TEAP (tetraethylammoniumperchlorate) as supporting electrolyte at 25 mV/s scan rate. The cyclic voltammogram of complex A (Figure 2a) showed two anodic peaks at $E^1_{p,a}$ = -0.27 V and $E^2_{p,a}$ = -0.60 V corresponds to cathodic peaks at $E^1_{p,c}$ = -0.37 V and $E^2_{p,c}$ = -0.85 V. The peak separation (ΔE = +0.10 V) and peak current ratio (0.92), for the first redox couple, suggested a quasi-reversible redox couple and can be featured to the Fe^{+2}/Fe^{+3} redox couple with the formal potential $E_{1/2}$ = -0.32 V. However, the second redox couple was found to be irreversible with large peak separation and asymmetric peak heights and can be attributed to the $Fe^{+1} \rightarrow Fe^{+2}$ process [23].

Further, the cyclic voltammogram of complex B (Figure 2b) also showed two anodic peaks at $E^1_{p,a}$ = +0.67 V and $E^2_{p,a}$ = -0.28 V corresponds to cathodic peaks at $E^1_{p,c}$ = +0.62 V and $E^2_{p,c}$ = -0.38 V. On account of peak separation (ΔE^1 = +0.05 V) and peak current ratio (0.94),

the first redox couple can be attributed to the reversible Co^{+2}/Co^{+3} redox couple. While, second redox couple can be allocated to quasi-reversible Co^{+2}/Co^{+1} redox couple as supported by ΔE^2 = +0.10 V and peak heights [23].

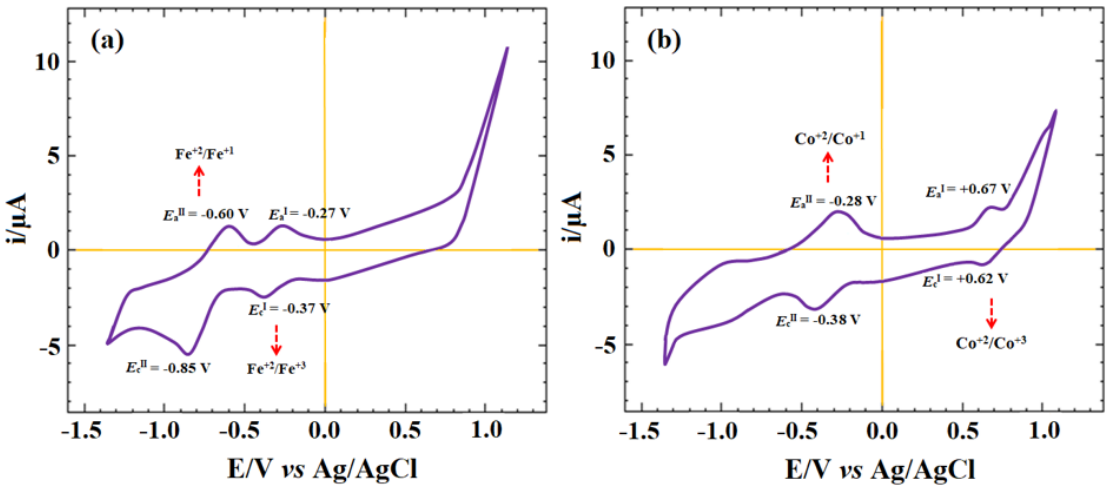

Fig. 2. Cyclic voltammogram of (a) A-Fe, and (b) B-Co macrocyclic complex, recorded in DMF (10^{-3} M) solution along with 0.1 M TEAP (tetraethylammoniumperchlorate) as supporting electrolyte under nitrogen atmosphere at 25 mVs^{-1} scan rate

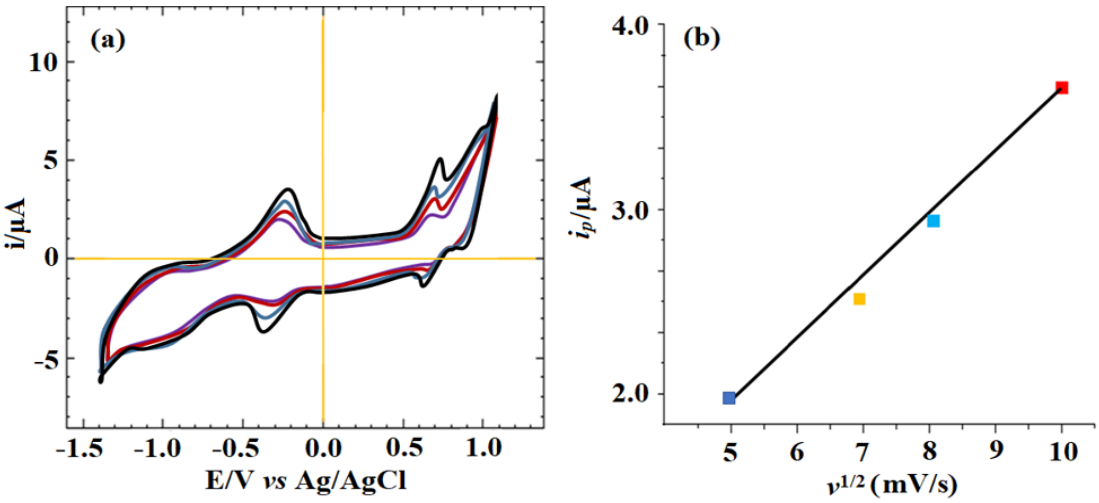

Fig. 3. (a) Cyclic voltammogram of complex B, recorded in DMF (10^{-3} M) solution along with 0.1 M TEAP (tetraethylammoniumperchlorate) as supporting electrolyte under nitrogen atmosphere, at different scan rates 25-100 mVs^{-1}, and (b) Plot of i_p vs $v^{1/2}$

Further, the CVs of both macrocycles were also recorded in DMF at different scan rate in the range of 25–100 mVs^{-1} and founded that $E_{p,a}$ and $E_{p,c}$ increase linearly with increasing scan rate. The cathodic peak potential shifted towards negative potential and the anodic peak shifted

towards positive potential. Thus, peak separation (ΔE) values increased, showing deviation of redox process from reversibility whereas peak current increase linearly that showed diffusion controlled process hence, follows Randles-Sevick equation (1) [24,25] (Figure 3a and b):

$$i = 2.69 \times 10^5 \, n^{3/2} A \, D^{1/2} \, c \, v^{1/2} \quad (1)$$

where n is the number of electrons transferred, A is the area of the electrode, D is the diffusion coefficient, c is the analyte concentration and v is the scan rate.

3.6. Catalytic Oxidation of Hydroquinone (H_2Q)

For the investigation of catalytic oxidation of H_2Q using the synthesized macrocycles, H_2Q (3 mmol) was dissolved in $CHCl_3$ (250 ml) solution of the macrocyclic complex (0.25 mmol). Then, O_2 was bubbled into the obtain slurry for 4 hrs with constant stirring at 30°C, the resulting slurry was filtered, concentrated with the help of rotary evaporator [26]. The obtained concentrate was employed at the top of a silica gel (60-120 mesh) column and eluted with CH_2Cl_2. This eluted material was evaporated to dryness using rotary evaporator, obtained solid material was recrystallized with petroleum ether to get the pure 1,4-benzoquinone (BQ) yellow needles. The BQ products were characterized by melting points and IR data (Table 3).

Table 2. Catalytic data of Oxidation of H_2Qs using synthesized Macrocycles

Analytical Data of various BQs products					
Substituent	Yield (%) 1,4-BQs	IR ν (C=O) cm^{-1}	Melting point (°C)		Ref.
			This study	literature	
-H	56	1662	111	113	[26]
2,3,5-$(CH_3)_3$	72	1639	31	31	[27]
-Cl	55	1655	56	57	[28]
-OCH_3	70	1634,1672	146	147	[29]
Yields of BQ product with macrocycles					
Catalyst		Used gas		Yield (%) 1,4-BQ	
A		air		25	
B		air		56	
No catalyst		air		00	
Yields of BQ product with various base					
B (mMol)		Base (mMol)		Yield (%) 1,4-BQ	
0.25		3,4-DAPy (3.0)		13	
0.25		Py (0.6)		30	
0.25		Py (6.0)		18	
0.25		No base		42	

Typically, both macrocycles of A and B were used for the catalysis of H_2Q in the presence of air as illustrated in Scheme 2. The H_2Q was added in a 12-fold over the catalyst. The results

in terms of yield (%) of BQ are given in Table 2, indicating the high specificity of complex B as compared to complex A toward this auto-oxidation. The catalytic activity of these macrocycles was evident as a blank experiment (with no catalyst) does not give the oxidative product at all[26]. Further, the catalytic activity of complex B seems to be dependent on the substrate as supported by the results in terms of yields; H_2Q gives only 44% yield of oxidative product 1,4-BQ, while chloro, methoxy, and 2,3,5-trimethyl substituted H_2Q gives 50%, 74% and 70% yield of corresponding BQs, respectively. Our results are in good agreement with the previously reported works [27,28].

Thus, it can be considered that the auto-oxidation of H_2Q is influenced by the electronic and/or steric effects exerted by the substituents on phenyl ring [30]. In addition, the results also suggested that the catalytic activity of macrocycles is a function of the nature of axial base additives and their concentrations. For example, the yield of 1,4-BQ was observed significantly low in the presence of pyridine (Py) and 3,4-diamino pyridine (DAPy) as axial bases (Table 3), it can be attributed to the coordination of N-atom of Py/DAPy with Co metal ion, reduce the catalytic efficiency.

Further, the catalytic oxidation may involve the dehydrogenation of BQs in terms of H-atom transfer to O atom for the formation of 1,4-benzoquinones and H_2O_2, however, no definite evidence for this mechanism can be given at this time. Our further study will focus on the investigation of the mechanism of this auto-oxidation of H_2Q into BQ using macrocycles.

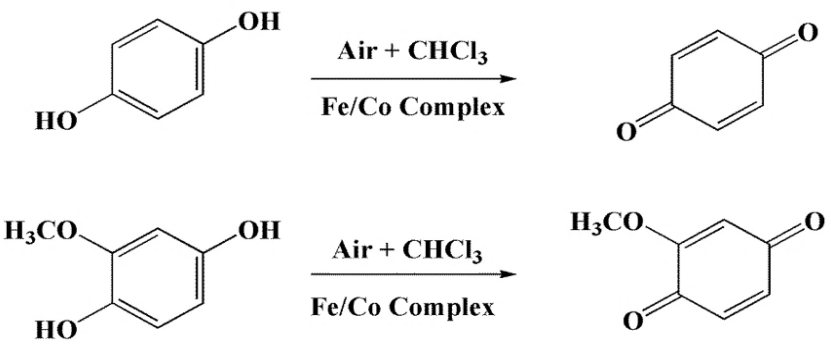

Scheme 2. The catalytic oxidation of H_2Qs into corresponding BQs in the presence of air

4. CONCLUSION

In the present investigation, tetraazamacrocycles of Fe^{III} and Co^{II} metal ions were blended by utilizing a template strategy. On the basis of spectral data and theoretical calculations, an octahedral with more saddle distortion geometry were assigned for these macrocycles. The electrochemical investigations of macrocycles demonstrated the adjustment of surprising oxidation conditions of relating metal ions. Further, the experimental consequences presented herein enlighten the catalytic oxidation of hydroquinone using the synthesized macrocycles. The findings proposed that the molecular oxygen is inert with H_2Q without the macrocycles.

However, the presence of these macrocycles demonstrated the critical synergist oxidation of hydroquinone. Further, Co^{II} tetraazamacrocyclic complex was observed to be a proficient impetus for the oxidation of H_2Q into relating BQ alongside the creation of H_2O_2. The catalytic efficiency seems to get enhanced by the presence of electron releasing groups in the aromatic ring. It might be because of the profoundly positive $Co^{2+/3+}$ potential windows. However, as of now, the mechanism isn't clear. Therefore, our next investigation will consider the component investigation of this synergist H_2Q oxidation response utilizing macrocycles. This work can be filled in as the engineered possibly macrocycles models and can be connected in different electrocatalysis.

Acknowledgments

We are thankful to GLA University, Mathura for infrastructural support and SAIF Panjab University Chandigarh for completion of the studies.

Conflicts of interest

There are no conflicts to declare.

REFERENCES

[1] R. E. Mewis, and S. J. Archibald, Coord. Chem. Rev. 254 (2010) 15.
[2] B. J. Kraft, N. L. Coalter, M. Nath, A. E. Clark, A. R. Siedle, J. C. Huffman, and J. M. Zaleski, Inorg. Chem. 42 (2003) 1663.
[3] M. Zhu, D. T. Yang, R. Ye, J. Zeng, N. Corbin, and K. Manthiram, Catal. Sci. Technol. 9 (2019) 974.
[4] J. Cho, R. Sarangi, and W. Nam, (2012). Acc. Chem. Res. 45 (2012) 1321.
[5] Z. Vargová, R. Gyepes, L. Arabuli, K. Györyová, P. Hermann, and I. Lukeš, (2009). Inorg. Chim. Acta 362 (2009) 3860.
[6] E. Musluoglu, A. Gürek, V. Ahsen, A. Gül, and O. Bekaroğlu, Eur. J. Inorg. Chem. 125 (2010) 2337.
[7] X. Zhang, Y. Zhu, X. Zheng, D. L. Phillips, and C. Zhao, Inorg. Chem. 53 (2014) 3354.
[8] H. Elias, Coord. Chem. Rev. 187 (1999) 37.
[9] L. F. Lindoy, Pure Appl. Chem. 61 (1989) 1575.
[10] A. N. Campbell, P. B. White, I. A. Guzei, and S. S. Stahl, J. Am. Chem. Soc. 132 (2010) 15116.
[11] S. D. McCann, and S. S. Stahl, Acc. Chem. Res. 48 (2015) 1756.
[12] V. K. Vashistha, and A. Kumar, Inorg. Chem. Comm. 112 (2020) 107700.
[13] P. U. Maheswari, F. Hartl, M. Quesada, F. Buda, M. Lutz, A. L. Spek, P. Gamez and J. Reedijk, Inorg. Chim. Acta, 374 (2011) 406.

[14] O. A. Ulloa, M. T. Huynh, c. P. Richers, J. A. Bertke, M. J. Nilges, S. Hammes-Schiffer, and T. B. Rauchfuss, J. Am. Chem. Soc. 138 (2016) 9234.
[15] L. E. Fernandez, S. Horvath, and S. Hammes-Schiffer, J. Phys. Chem. Lett. 4 (2013) 542.
[16] A. Kumar, V. K. Vashistha, P. Tevatia, and R. Singh, Spectrochim. Acta A 176 (2017) 123.
[17] S. Chandra, Spectrochim. Acta A 103 (2013) 338.
[18] S. Chandra, D. Jain, and A. K. Sharma, Spectrochim. Acta A 71 (2009) 1712.
[19] I. P. Beletskii, and K. B. Yatsimirskii, Theor. Exp. Chem. 20 (1985) 483.
[20] A. Kumar, V. K. Vashistha, P. Tevatia, and R. Singh, Der. Pharma. Chemic. 8 (2016) 146.
[21] K. S. Siddiqi, A. Jabeen, N. Kishat, and S. A. A. Zaidi, Synth. React. Inorg. Met. Org. Chem. 23 (1993) 735.
[22] P. M. Reddy, R. Rohini, E. R. Krishna, A. Hu, and V. Ravinder, Int. J. Mol. Sci. 13 (2012) 4982.
[23] Sweety, V. K. Vashistha, A. Kumar and R. Singh, Russ. J. Electrochem. 55 (2019) 161.
[24] Y. W. D. Chen, and A. J. Bard, Inorg. Chem. 23 (1984) 2175.
[25] A. Kumar, V. K. Vashistha, P. Tevatia and R. Singh, Anal. Bioanal. Electrochem, 8 (2016) 848.
[26] A. Kumar and R. Singh, Anal. Bioanal. Electrochem. 8 (2016) 382.
[27] M. J. Hostetler, S. J. Green, J. J. Stokes, and R. W. Murray, J. Am. Chem. Soc. 118 (1996) 4212.
[28] E. R. I. C. H. Dorn, and H. J. Knackmuss, Biochem. J. 174 (1978) 85.
[29] C. Balraj, A. Satheshkumar, K. Ganesh, and K. P. Elango, RSC Adv. 2 (2012) 12384.
[30] K. Ganesh, C. Balraj, A. Satheshkumar, and K. P. Elango, Spectrochim. Acta Part A 92 (2012) 46.